Diffusion tensor imaging of the corpus callosum: a cross-sectional study across the lifespan

Nicole C.R. McLaughlin [a,*], Robert H. Paul [b], Stuart M. Grieve [c], Leanne M. Williams [d,e,h],
David Laidlaw [f], Margaret DiCarlo [a], C. Richard Clark [g], William Whelihan [a],
Ronald A. Cohen [a], Thomas J. Whitford [d,e], Evian Gordon [c,d]

[a] *Brown Medical School, Department of Psychiatry and Human Behavior, Box G-BH, Providence, RI 02912, USA*
[b] *Behavioral Neuroscience, Department of Psychology, University of Missouri, St. Louis, USA*
[c] *The Brain Resource International Database, The Brain Resource Company, Ultimo, NSW 2007, Australia*
[d] *Brain Dynamics Centre, Westmead Millenium Institute, Westmead Hospital, USA*
[e] *Department of Psychological Medicine, University of Sydney, Australia*
[f] *Brown University, Department of Computer Science, USA*
[g] *Cognitive Neuroscience Laboratory and School of Psychology, Flinders University, Adelaide, SA 5001, Australia*
[h] *School of Psychology, University of Sydney, Australia*

Abstract

Previous studies have demonstrated strong developmental trends of white matter using in vivo neuroimaging. However, few studies have examined white matter using diffusion tensor imaging across the lifespan. In the present study we examined fractional anisotropy and volume in the corpus callosum in four groups (children, adolescents, young adults, and elderly). Results revealed a curvilinear relationship in the analysis of the fractional anisotropy values for these four groups, with fractional anisotropy values increasing in childhood and adolescence, reaching their peak in young adulthood, followed by a non-significant decline in the elderly. Volumetric analysis of corpus callosum regions revealed a similar pattern, with an increase in volume from childhood and adolescence through young adulthood, and a non-significant decrease in volume in the elderly group. These results define the microstructural development of the white matter across the lifespan. Future studies are required to examine the neurobehavioral correlates of these neuroimaging indices.
© 2007 Published by Elsevier Ltd on behalf of ISDN.

Keywords: Diffusion tensor; Neuroimaging; Lifespan; Development; Corpus callosum; White matter

Several research studies, including work from members of this research group (Grieve et al., 2007), have reported significant developmental trends of the brain white matter ultrastructure using diffusion tensor imaging (DTI; McGraw et al., 2002; Snook et al., 2005; Ben Bashat et al., 2005; Li and Noseworthy, 2002). DTI is a relatively new, non-invasive imaging technique that defines the rate and directionality of water diffusion in the brain parenchyma. Since water diffusion occurs preferentially along rather than across cells with a high degree of linear orientation, DTI is ideally suited to study white matter development. One principal scalar metric of DTI is fractional anisotropy, which provides an index of directionally dependent diffusion (Pierpaoli and Basser, 1996). In our own previous work we have demonstrated very strong relationships between age and FA in the white matter among healthy individuals (Grieve et al., 2007).

FA increases rapidly in early life, representing increasing white matter myelination (McGraw et al., 2002; Snook et al., 2005). Studies have demonstrated that FA reaches an asymptote in the second or third decade of life (Ben Bashat et al., 2005; Li and Noseworthy, 2002). Subsequent to the stabilization of white matter development in early adulthood, the integrity of the white matter breaks down with advanced age, and this process is hypothesized to recapitulate the initial developmental process (Charlton et al., 2006; Pfefferbaum et al., 2000, 2005; Salat et al., 2005). Previous studies of cognition in the elderly have demonstrated that some select cognitive skills decline to pre-adolescent levels of proficiency (Clark et al.,

N.C.R. McLaughlin et al. / Int. J. Devl Neuroscience xxx (2007) xxx–xxx

2006). This decrease in FA in advanced age is especially pronounced in adults in their seventh and eighth decades of life (Nusbaum et al., 2001; Charlton et al., 2006) and the frontal regions of the brain are especially vulnerable to this degenerative process (Grieve et al., 2005; Nusbaum et al., 2001; Pfefferbaum et al., 2005; Salat et al., 2005). In the corpus callosum, age-related decline has been shown to be specific to the genu (Abe et al., 2002). These findings are consistent with other studies demonstrating age-related declines in white matter integrity. For example, quantitative MR studies have shown white matter volume decreases in the sixth decade of life with an absence of concurrent decrease in gray matter (Guttmann et al., 1998). There is also a decrease in white matter nerve fiber length and diameter in the elderly (Tang et al., 1997). Few research studies have examined developmental trends across the lifespan. However, correlations have been found in brain parenchymal volume between age (from childhood to elderly) and mean and peak height of the apparent diffusion coefficient, and fractional anisotropy peak height (Rovaris et al., 2003).

While the above studies have identified developmental trends in white matter integrity in younger and older cohorts, to our knowledge, no study has compared these developmental effects across the lifespan within the corpus callosum, including both young children and older adults. In the present study we used DTI and standard MRI techniques (T1- and T2-weighted imaging) to examine the corpus callosum among four groups of healthy individuals, including children, adolescents, young adults and older adults. With this multimodality dataset we used a novel technique for parcellating the CC, allowing an analysis of trends across the lifespan of volume measures and of structural WM integrity using the FA metric. Of particular interest in the present study was the degree to which FA decreased in the elderly in comparison to younger individuals, including children.

1. Experimental procedures

1.1. Participants

The participants in this study were healthy subjects participating in the Brain Resource International Database (BRID; Gordon, 2003). DTI and structural imaging data were available from individuals between the ages of 7 and 79. Only subjects with a full DTI and structural imaging dataset were included in this study. Four groups of healthy volunteers were used, including 10 children aged 7–12 years ($M = 10.0$, S.D. $= 1.76$), 36 adolescents aged 13–18 years ($M = 15.4$, S.D. $= 1.86$), 25 young adults aged 25–40 years ($M = 30.5$, S.D. $= 4.64$), and 11 elderly adults aged 60–80 years ($M = 65.4$, S.D. $= 4.20$). Participants were excluded if they had a personal history of mental illness (as assessed by the SPHERE, Hickie et al., 1998), physical brain injury, neurological disorder or other serious medical condition, or a personal history of drug or alcohol addiction. Participants were further excluded if they had a family history of Attention Deficit Hyperactivity Disorder (ADHD), Schizophrenia, or Bipolar Disorder. All participants gave informed consent and guardian consent was obtained for all participants under 18 years of age.

1.2. MRI acquisition

Magnetic Resonance Images were acquired using a 1.5 T S (Erlangen, Germany) Sonata at Perrett Imaging, Flinders University, Australia. 3D T1-weighted images were acquired in the sagittal plane using a 3D MPRAGE sequence (TR = 9.7 ms; TE = 4 ms; Echo train: 7; flip angle = 12°; TI = 200 ms; NEX = 1). A total of 180 contiguous 1 mm slices were acquired with a 256×256 matrix with an in plane resolution of 1 mm $\times$ 1 mm resulting in isotropic voxels. Proton density and T2-weighted (T2W) images were acquired using a dual echo sequence (TR: 7530 ms; TE: 15/105 ms; Echo train: 7; flip angle: 180°; NEX: 1). 45 contiguous 1 mm slices are acquired in an axial orientation with an in-plane matrix of 256×256 at a resolution of 0.86 mm $\times$ 0.86 mm. Diffusion tensor images (DTI) were acquired using a DTI-EPI sequence (TR: 160 ms; effective TR: 5.120 s; TE: 88 ms; fat saturation; NEX: 4). A baseline image ($b = 0$) and 12 different diffusion orientations were acquired with a b-value of 1250. The diffusion gradient encoding scheme was as follows: $(x,y,z) = [(1,0,0.5),$ $(0,0.5,1),$ $(0.5,1,0),$ $(1,0.5,0),$ $(0,1,0.5),$ $(0.5,0,1),$ $(1,0,-0.5),$ $(0,-0.5,1),$ $(-0.5,1,0),$ $(1,-0.5,0),$ $(0,1,-0.5),$ $(-0.5,0,1)]$. Thirty-two contiguous slices of 6.5 mm were acquired with an in-plane matrix of 128×128 at a resolution of 1.72 mm $\times$ 1.72 mm. Fractional anisotropy (FA) was the principal DTI metric for the present study. FA represents the degree of anisotropic diffusion present in each image voxel. The primary region of interest was the corpus callosum, which was further divided into three sub-regions: the genus, body, and splenium of the corpus callosum.

1.3. Diffusion tensor analysis

DTI data was processed using a custom written routine (by author—SMG) in MATLAB 6.5 (MathWorks, Natick, USA). Trace apparent diffusion co-efficient (TrADC) and FA images were calculated in native space from the $b = 0$ image and 12 diffusion weighted imaged images ($b = 1250$ s cm^{-2}). FA was defined as:

$$FA = \left(\frac{3}{2}\right)^{1/2} \times \left[\frac{(\lambda_1 - \lambda_{av})^2 + (\lambda_2 - \lambda_{av})^2 + (\lambda_3 - \lambda_{av})^2}{\lambda_1^2 + \lambda_2^2 + \lambda_3^2} \right]^{1/2}$$

where λ_n is the eigenvalues describing the diffusion tensor, and λ_{av} is the mean diffusivity $((\lambda_1 + \lambda_2 + \lambda_3)/3)$.

1.4. Corpus callosum parcellation

A hand-drawn region of interest was drawn using an normalized, averaged and high resolution (1 mm^3) smoothed WM segmented image created from 223 individuals from the BRID dataset in a previous work (Grieve et al., 2005). The position of the division between the anterior portion of the genu and the frontal pericallosal tissue, and between the postero-lateral extent of the splenium and the parietal pericallosal tissue was defined by a plane positioned bordering the medial 30% of the brain diameter as described by Pfefferbaum et al. (2000). With this position demarked in an axial view a line perpendicular to the long axis of the lateral extent of the genu or splenium was drawn. Fig. 1 shows the position of the CC ROI superimposed on a segmented WM image calculated using T1-weighted data (see below); the divisions of the CC into the genu, body and splenium are shown in Fig. 1g. In order to smooth the ROI prior to use, a 4 mm Gaussian filter was then applied and the ROI borders redefined according to a threshold of 50% of maximum intensity. The genu was defined as the portion of the CC ROI anterior to a plane through the body of the CC at the MNI co-ordinate $y = 17$ mm. The splenium was defined as the portion of the CC posterior to a plane at the MNI co-ordinate $y = -18$ mm (Fig. 1g).

1.5. Segmentation of T1 MRI data

Co-registration and normalization was performed using Statistical Parametric Mapping (SPM2; Wellcome Department of Imaging Neuroscience, London; http://www.fil.ion.ucl.ac.uk/spm), running under MATLAB 6.5 using an optimized VBM protocol at a resolution of 1 mm^3. The details of this procedure have been SPM as previously described (Ashburner and Friston, 2000; Good et al., 2001; Grieve et al., 2005). The segmentation protocol used a cluster analysis method to separate pixels based on intensity differences, together with a priori knowledge of spatial tissue distribution patterns in normal subjects (Ashburner and Friston, 2000; Friston et al., 1996; Good et al., 2001). Customized GM, WM and CSF template images were created from the averaged T1 images of 223 individuals in the BRID database (Grieve et al., 2005). The final step of this protocol involved normalizing segmented WM data to a target high resolution, smoothed WM template.
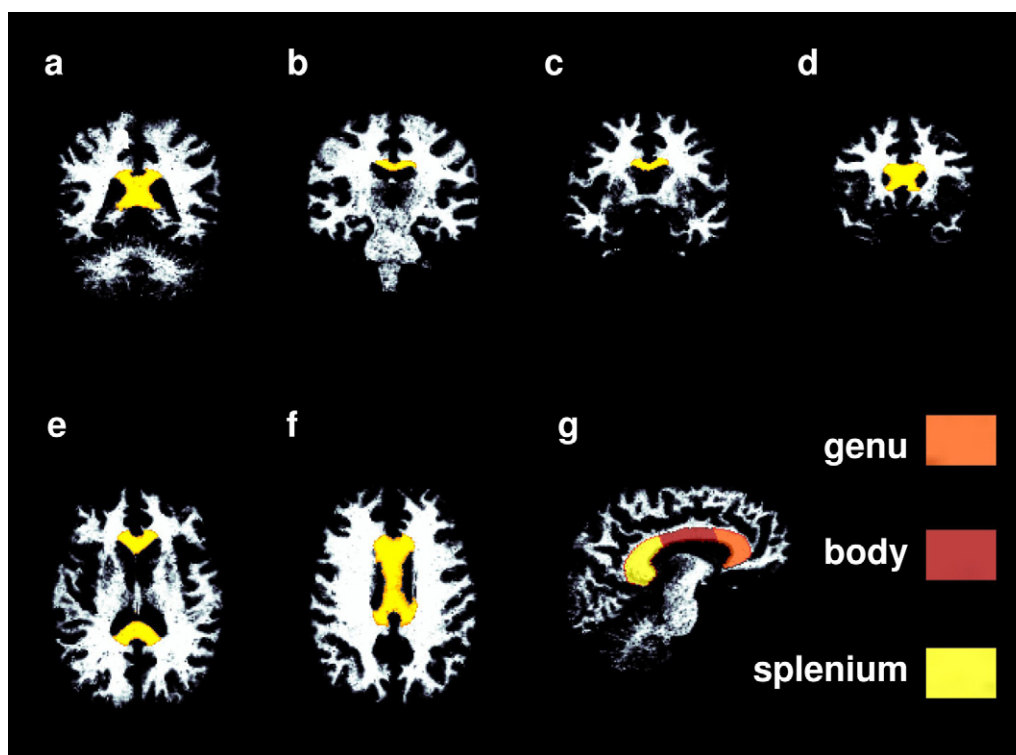
Fig. 1. A series of segmented WM images generated from T1-weighted data showing the localization of the corpus callosum (CC) region of interest. The location of the CC is shown in yellow in a–f, and yellow, red and orange in g. (a–d) Coronal sections caudal to rostral showing the splenium (a), body (b and c) and genu of the CC. (e and f) Axial slices showing (e) the inferior portions of the genu and splenium, and (f) the mid-portion of the CC through the bulk of the body. (g) A sagittal slice showing the subdivisions of the CC in color code. The genu is represented as orange, the body as red and the splenium as yellow. (For interpretation of the references to color in this figure legend, the reader is referred to the web version of the article.)

1.6. Creation of custom CC masks for FA and volume analysis

Following segmentation and normalization of the WM of each subject image to MNI space, the standard CC ROI masks were masked using a threshold of WM probability >0.4, so as to only include WM voxels. The WM data and the modified CC ROI masks were transformed back into "native" T1 space using the inverse of the deformation fields created through the normalization process (Deformation Toolbox, SPM2, John Ashburner). At this point WM volume was calculated for each CC ROI using the segmented WM data in native space and the CC masks (see Fig. 1). The native T1 image was then co-registered to the T2 dataset, in the process resampling to the 3 mm slice thickness of the T2 data. The T2 data was then co-registered to the calculated TrADC image—this image pair was chosen for this spatial transform as best results were obtained in iterative testing (data not shown). The transforms from these two steps were then used to morph both the segmented WM data and the CC masks to the native space of the DTI dataset. Fig. 2a shows FA maps from four axial slices from a representative individual. In Fig. 2b the segmented WM masks are superimposed in color over these FA images (Fig. 2b), and in Fig. 2c the CC ROIs are similarly superimposed (Fig. 2c). Average FA values were then calculated using both the custom CC masks and the segmented WM mask to ensure WM only was analyzed. Fig. 1b–d shows a representative CC mask superimposed on a T1 (Fig. 1b), T2 (Fig. 1c) and FA dataset (Fig. 1d).

1.7. Statistical analyses

A univariate analysis of variance (ANOVA) was conducted, with age group (children, adolescents, young adults, elderly) as the independent variable, and volume and FA of the total corpus callosum, as well as the sub-regions of the corpus callosum (i.e. genu, body and splenium) as the dependent variables. Tukey's least squared differences test was used for post hoc comparisons, and accounted for multiple comparisons.

2. Results

2.1. Fractional anisotropy

Over the whole CC, FA followed an inverted-'U' trend with FA values increasing from childhood (FA = 0.35), through adolescence (FA = 0.47), to young adulthood (FA = 0.57) and a decrease in the elderly (FA = 0.47). There was a significant difference between groups in the FA of the entire corpus callosum ($F(3, 78) = 8.19$, $p < 0.001$; see Table 1; Fig. 3). Specifically, the youngest group exhibited significantly lower FA in the whole corpus callosum compared to the adolescents ($p < 0.05$) and the young adults ($p < 0.001$). Adolescents also had significantly lower FA values in comparison to the young adults ($p < 0.05$), indicating continued overall development of the corpus callosum from adolescence to young adulthood. There were no significant differences in the FA of the entire corpus callosum between the elderly and the young adults, adolescents, or children in any of the studied age ranges. Visual examination of the mean values reveals very similar values of FA in the entire corpus callosum in the elderly group compared to the adolescent group.

The trends described above for the whole CC are replicated for each of the three components of the CC. Significant differences in FA were found between groups in the genu of the corpus callosum ($F(3, 78) = 4.77$, $p < 0.01$; see Table 1; Fig. 4). Post hoc analyses showed lower FA values in the
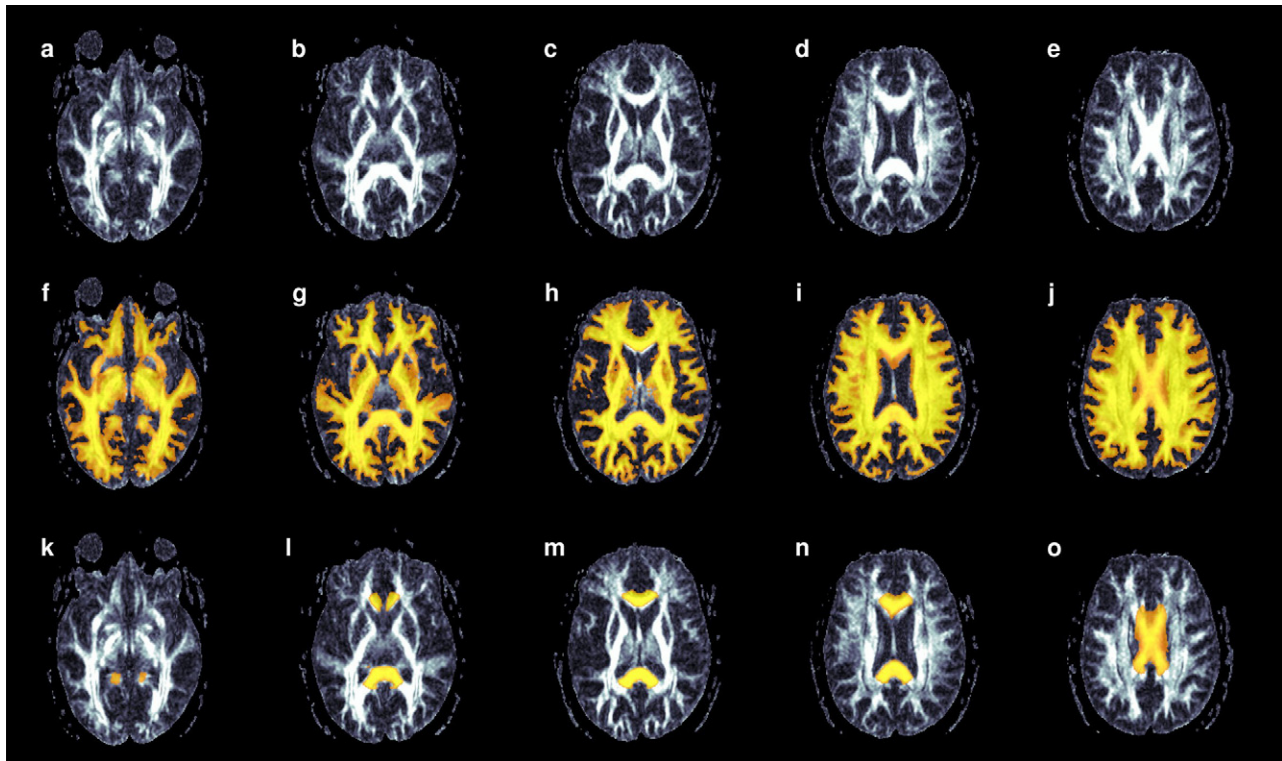
Fig. 2. Axial slices of a representative subject showing: (a–e) fractional anisotropy (FA) images arranged in a inferior to superior direction. (f–j) FA images with segmented WM data superimposed in color. WM data is calculated from T1-weighted images in MNI space, and warped to FA-native space via a series of transforms that involve co-registering T1-weighted, T2-weighted, apparent diffusion co-efficient and FA images. (k–o) Corpus callosum ROIs superimposed onto the FA images. ROIs are defined in MNI space, then warped to FA-native space as described above. (For interpretation of the references to color in this figure legend, the reader is referred to the web version of the article.)

children as compared to the young adults ($p < 0.01$), but insignificant differences among the other group comparisons.

There were also significant between group differences in the FA values for the body of the corpus callosum ($F(3, 78) = 6.81$, $p < 0.001$; see Table 1). Post hoc analyses of FA values in the body of the corpus callosum showed significant differences between the children and the young adults ($p < 0.001$), and the adolescents and the young adults ($p < 0.05$), with the values for
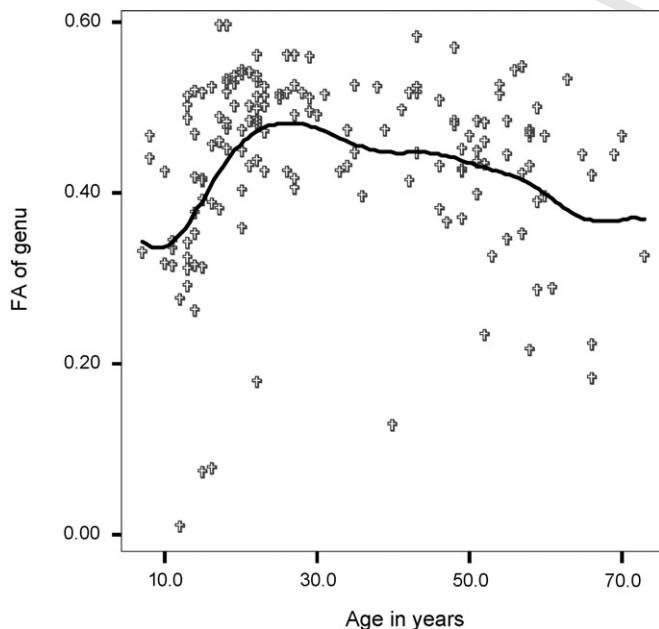

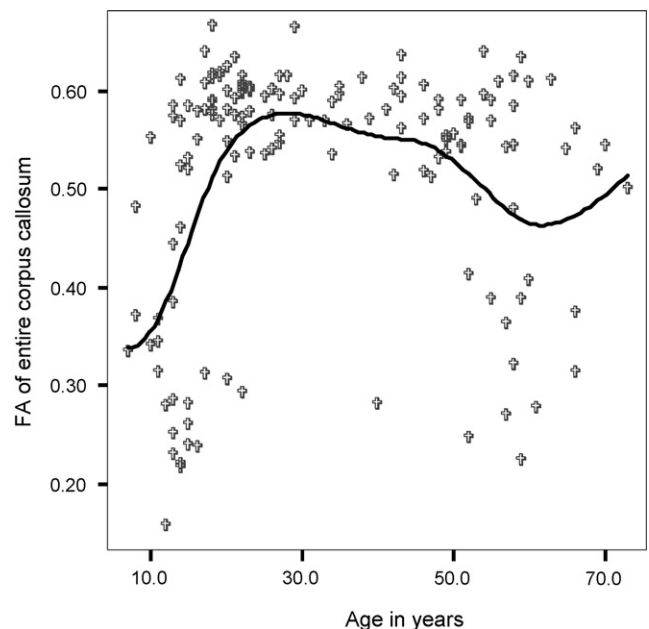
Fig. 3. FA vs. age in the genu of the corpus callosum.

Fig. 4. FA vs. age in the entire corpus callosum.

Table 1
Group analysis statistics [*M*(S.D.)] for FA of corpus callosum (CC)

Region	Children (*N* = 10; 7–12 years)	Adolescents (*N* = 36; 13–18 years)	Young adults (*N* = 25; 25–40 years)	Elderly (*N* = 11; 60–80 years)	*F*	*p*
Entire CC	0.35 (0.11)	0.47 (0.15)	0.57 (0.07)	0.47 (0.12)	8.19	<0.001
Body of CC	0.35 (0.12)	0.48 (0.17)	0.58 (0.09)	0.50 (0.15)	6.81	<0.001
Genu of CC	0.32 (0.13)	0.41 (0.12)	0.47 (0.09)	0.37 (0.11)	4.77	0.004
Splenium of CC	0.37 (0.12)	0.50 (0.18)	0.61 (0.06)	0.51 (0.13)	7.70	<0.001

Table 2
Group analysis statistics [*M*(S.D.)] for volume of corpus callosum (CC)

Region	Children (*N* = 10; 7–12 years)	Adolescents (*N* = 36; 13–18 years)	Young adults (*N* = 25; 25–40 years)	Elderly (*N* = 11; 60–80 years)	*F*	*p*
Entire CC (mL)	14.47 (2.42)	17.59 (2.90)	18.53 (3.54)	18.19 (2.20)	4.60	0.005
Body of CC (mL)	3.19 (0.60)	4.13 (0.85)	4.37 (0.86)	4.44 (0.46)	6.08	0.001
Genu of CC (mL)	4.80 (0.86)	5.47 (0.81)	5.66 (1.27)	5.28 (0.76)	1.95	0.129
Splenium of CC (mL)	6.48 (1.01)	7.99 (1.38)	8.51 (1.55)	8.47 (1.27)	5.54	0.002

the young adult group being significantly higher than the values for the children or adolescents. There were no significant differences in the FA of the body of the corpus callosum between the children and adolescents, or the elderly from any of the groups.

FA values in the splenium of the corpus callosum also showed significant differences across groups ($F(3, 78) = 7.70$, $p < 0.001$; see Table 1). The children showed significantly lower FA values in comparison to the adolescents ($p < 0.05$) and young adults ($p < 0.001$). FA values for the adolescents were also significantly lower than those for the young adults ($p < 0.05$), but there were no significant differences in FA between the other groups.

2.2. Volumetric analyses

Volume changes in the whole CC showed an increase from childhood (WM volume = 14.5 mL) to young adulthood (WM volume adolescence = 17.6 mL; WM volume young adulthood = 18.5 mL), followed by a plateau with advancing age (WM volume 18.2 mL). There was a significant difference between groups in the total volume of the corpus callosum ($F(3,78) = 4.60$, $p < 0.01$; see Table 2). Post hoc analyses of the total corpus callosum volume showed that the children had significantly lower values in comparison to the adolescents ($p < 0.05$), the young adults ($p < 0.01$), and the elderly ($p < 0.05$). There were no significant differences across the other groups.

There were also significant differences between groups in the volumes of the body of the corpus callosum ($F(3, 78) = 6.08$, $p = 0.001$; see Table 2), with the children exhibiting lower values than the adolescents ($p < 0.01$), young adults ($p = 0.001$), and the elderly ($p < 0.01$). There were no significant differences between the other groups.

Consistent with the total volume and the volume of the body, in the splenium of the corpus callosum, ANOVA's indicated significant differences between groups ($F(3, 78) = 5.54$, $p < 0.01$; see Table 2). There were significant differences between the children and adolescents ($p < 0.05$), children and young adults ($p = 0.001$), and children and elderly ($p < 0.01$), with the children consistently having lower values. There were no differences between the other groups.

3. Discussion

In the present study we identified a curvilinear relationship between FA and age, with FA values increasing in childhood and adolescence, reaching their peak in young adulthood, and showing a non-significant decline in the elderly. The elderly group generally showed a similar profile to the adolescent group, and was not significantly different from the children in terms of diffusion within the white matter. Remarkably, the absolute FA values in the genu between the youngest group (average age = 10) and the oldest group (average age = 65) was nearly identical (0.31 and 0.37 respectively) revealing a similar degree of white matter integrity in the children and oldest adults. Our results also support a curvilinear relationship in the volume of the splenium and of the entire corpus callosum, with an increase in volume from childhood and adolescence through young adulthood, plateauing with a non-significant decrease in volume in the elderly group.

This research supports past studies of white matter maturation and later degeneration. Although there has been scarce research integrating white matter changes across the lifespan, previous research has demonstrated a curvilinear relationship in FA in the genu of the corpus callosum, with an increase until adulthood, with a subsequent decrease, similar to the current findings. Contrary to the current findings, this study did not find a similar relationship in the splenium, but rather found that the splenium FA was age-independent (Hasan et al., 2004); this difference may be accounted for by differing age groups and sectioning of the corpus callosum. The increase in the volume and the FA of these regions in the corpus callosum supports ongoing white matter maturation, with a likely corresponding increase in myelination, from early childhood

until young adulthood. Subsequently there appears to be a mild loss of white matter and possibly demyelination in the span between young adulthood and the elderly. FA may be a more sensitive measure of white matter changes. In this study, for example, there was a (non-significant) mild decrease in FA values with a corresponding (non-significant) increase in white matter volume in the body of the corpus callosum. FA may be sensitive to changes in myelination or coherence in this region, with no loss in white matter volume.

Given that the corpus callosum is the primary pathway for inter-hemispheric communication, it is reasonable to expect an association between its development and the development of cognitive processes. Analysis of microstructural integrity may be more sensitive to subtle changes in white matter that may affect cognition. There have been few studies completed examining the relationship between development of cognitive functions and the relationship to FA values. In children, studies have shown a relationship between cognitive tasks, such as reading, working memory, and intelligence, and FA in different regions, without examining the relationship with age (Beaulieu et al., 2005; Schmithorst et al., 2005). Development of working memory capacity as well as the development of reading ability has been shown to have a correlation with FA in the left frontal lobe. When the effect of age was removed, some of the relationships lost their significance, indicating that the impact of development is especially important in those regions (left superior fronto-parietal cluster for working memory, left temporal white matter cluster for reading; Nagy et al., 2004).

In adults, prior studies have demonstrated a relationship between FA values and performance on multiple cognitive tasks. In elderly adults, there is a relationship between FA in several regions of interest (premotor/pericallosal bundle, postcentral bundle, posterior parietal bundle, superior temporal bundle) and sections of the Stroop task, with higher FA values leading to better performance (Sullivan et al., 2005). Correlations have been found between working memory, executive functions, and speed, and FA values in whole brain white matter and anterior, middle, and posterior white matter regions (Charlton et al., 2006). FA values in the frontal white matter are significantly correlated with reaction time, and larger correlations have been found between FA values in the centrum semiovale and performance on the MMSE, and other areas of cognitive functioning and information processing (Deary et al., 2006). Relationships have also been found between measures of executive functioning and FA throughout the frontal, parietal, and temporal lobes, and are especially significant in the prefrontal cortex (Grieve et al., 2007).

There are several limitations to this research. The study is of a cross-sectional nature, and therefore is extrapolating lifespan data across multiple cohorts; a longitudinal study may better address the question of white matter development across the lifespan. Each group had a relatively small number of participants, which may reduce the statistical power of the analyses. An important methodological limitation of our study is the potential for partial volume effects due to the relative coarseness of the DTI dataset (6.5 mm slice thickness. Although our methods of defining the ROIs incorporated information from high-resolution T1- and T2-weighted data,) that allow the placement of ROIs with great fidelity, the raw slice thickness may introduce some partial volume errors that may reduce the sensitivity of our analysis, or worse, introduce some systematic bias. In addition, a limited number of brain regions were studied. It is possible that there is a different pattern of microstructural development in other brain regions, and that the development and decline of the corpus callosum is not generalizable across the cerebrum. Specifically, regions of gray matter were not analyzed, and these regions may have a different developmental trajectory than white matter regions.

The development of diffusion tensor imaging has supplied a new method with which to study the human brain. Recent research has shown that DTI may be more sensitive than conventional MRI techniques, especially when examining neurological disorders (Ge et al., 2005; Sundgren et al., 2004). Future studies are certainly forthcoming in utilizing DTI to study the development and decline of brain structures across the lifespan, in both gray as well as white matter. Examining a longitudinal group of participants to address this research question would be especially prudent. Larger group sizes would aid in increasing the statistical power of the results. Other regions of the brain, both in white and gray matter, should be studied in order to determine the developmental differences of various areas. The addition of the study of cognition in relationship to the development of neuroanatomical regions would be especially relevant to the field of behavioral neuroscience. It is also possible that the development of these brain regions takes a different path in various clinical populations, and research into these differences may aid in assessment and treatment options.

In conclusion, structural MRI and diffusion tensor imaging both show a similar, curvilinear pattern of white matter development across the lifespan in the entire corpus callosum and its constituent structures. This result is consistent with previous research demonstrating an increase in FA and total amount of white matter throughout the lifespan, with a decrease in old age.

Acknowledgements

References

Abe, O., Aoki, S., Hayashi, N., Yamada, H., Kunimatsu, A., Mori, H., Yoshikawa, T., Okubo, T., Ohtomo, K., 2002. Normal aging in the central nervous system: quantitative MR diffusion-tensor analysis. Neurobiol. Aging 23, 433–441.

Ashburner, J., Friston, K.J., 2000. Voxel-based morphometry—the methods. NeuroImage 11, 805–821.

Beaulieu, C., Plewes, C., Paulson, L.A., Roy, D., Snook, L., Concha, L., Phillips, L., 2005. Imaging brain connectivity in children with diverse reading ability. NeuroImage 25, 1266–1271.

Ben Bashat, D.B., Sira, L.B., Graif, M., Pianka, P., Hendler, T., Cohen, Y., Assaf, Y., 2005. Normal white matter development from infancy to adulthood: comparing diffusion tensor and high *b* value diffusion weighted MR images. J. Magn. Reson. Imaging 21, 503–511.

Charlton, R.A., Barrick, T.R., McIntyre, D.J., Shen, Y., O'Sullivan, M., Howe, F.A., Clark, C.A., Morris, R.G., Markus, H.S., 2006. White matter damage on diffusion tensor imaging correlates with age-related cognitive decline. Neurology 66, 217–222.

Clark, C.R., Paul, R.H., Williams, L.M., Arns, M., Fallahpour, K., Handmer, C., Gordon, E., 2006. Standardized assessment of cognitive functioning during development and aging using an automated touchscreen battery. Arch. Clin. Neuropsychol..

Deary, I.J., Baston, M.E., Pattie, A., Clayden, J.D., Whalley, L.J., Starr, J.M., Wardlaw, J.M., 2006. White matter integrity and cognition in childhood and old age. Neurology 66, 505–512.

Friston, K.J., Holmes, A., Poline, J.B., Price, C.J., Frith, C., 1996. Detecting activations in PET and fMRI: levels of inference and power. NeuroImage 4, 223–235.

Ge, Y., Law, M., Grossman, R.I., 2005. Applications of diffusion tensor MR imaging in multiple sclerosis. Ann. N.Y. Acad. Sci. 1064, 202–219.

Good, C.D., Johnsrude, I.S., Ashburner, J., Henson, R.N.A., Friston, K.J., Frackowiak, R.S.J., 2001. A voxel-based morphometric study of ageing in 465 normal adult human brains. NeuroImage 14, 21–36.

Gordon, E., 2003. Integrative neuroscience and psychiatry. Neuropsychopharmacology 28, S2–S8.

Grieve, S.M., Clark, C.R., Williams, L.M., Peduto, A.J., Gordon, E., 2005. Preservation of limbic and paralimbic structures in aging. Hum. Brain Mapp. 25, 391–401.

Grieve, S.M., Williams, L.M., Paul, R.H., Clark, C.R., Gordon, E., 2007. Cognitive aging, executive function and fractional anisotropy: a diffusion tensor MR Imaging study. Am. J. Neuroradiol. 28, 226–235.

Guttmann, C.R.G., Jolesz, F.A., Kikinis, R., Killianym, R.J., Moss, M.B., Sandor, T., Albert, M.S., 1998. White matter changes with normal aging. Neurology 50 (4), 972–978.

Hasan, K.M., Kanabar, B.P., Santos, R.M., Ewing-Cobbs, L., Narayana, P.A., 2004. Age dependence of the fractional anisotropy of genu and splenium of human corpus callosum using optimized DT-MRI. In: Proceedings of the International Society of Magnetic Resonance Medicine, vol. 11. p. 338.

Hickie, I., Hadzi-Pavlovic, D., Scott, E., Davenport, T., Koschera, A., Naismith, S., 1998. SPHERE: a national depression project. Australas. Psychiatry 6, 248–250.

Li, T., Noseworthy, M.D., 2002. Mapping the development of white matter tracts with diffusion tensor imaging. Dev. Sci. 5 (3), 293–300.

McGraw, P., Liang, L., Provenzale, J.M., 2002. Evaluation of normal age-related changes in anisotropy during infancy and childhood as shown by diffusion tensor imaging. Am. J. Roentgenol. 179, 1515–1522.

Nagy, Z., Westerberg, H., Klingberg, T., 2004. Maturation of white matter is associated with the development of cognitive functions during childhood. J. Cogn. Neurosci. 16, 1227–1233.

Nusbaum, A.O., Tang, C.Y., Buchsbaum, M.S., Wei, T.C., Atlas, S.W., 2001. Regional and global changes in cerebral diffusion with normal aging. Am. J. Neuroradiol. 22, 136–142.

Pfefferbaum, A., Adalsteinsson, E., Sullivan, E.V., 2005. Frontal circuitry degradation marks healthy adults again: evidence from diffusion tensor imaging. NeuroImage 26, 891–899.

Pfefferbaum, A., Sullivan, E.V., Hedehus, M., Lim, K.O., Adalsteinsson, E., Moseley, M., 2000. Age-related decline in brain white matter anisotropy measured with spatially corrected echo-planar diffusion tensor imaging. Magn. Reson. Med. 44, 259–268.

Pierpaoli, C., Basser, P.J., 1996. Toward a quantitative assessment of diffusion anisotropy. Magn. Reson. Med. 36, 893–906.

Rovaris, M., Iannucci, G., Cercignani, M., Sormani, M.P., De Stefano, N., Gerevini, S., Comi, G., Filippi, M., 2003. Age-related changes in conventional, magnetization transfer, and diffusion-tensor MR imaging findings: study with whole-brain tissue histogram analysis. Radiology 227, 731–738.

Salat, D.H., Tuch, D.S., Hevelone, N.D., Fischl, B., Corkin, S., Rosas, H.D., Dale, A.M., 2005. Age-related changes in prefrontal white matter measured by diffusion tensor imaging. Ann. N.Y. Acad. Sci. 1064, 37–49.

Schmithorst, V.J., Wolke, M., Dardzinski, B.J., Holland, S.K., 2005. Cognitive functions correlate with white matter architecture in a normal pediatric population: a diffusion tensor MRI study. Hum. Brain Mapp. 26, 139–147.

Snook, L., Paulson, L., Roy, D., Phillips, L., Beaulieu, C., 2005. Diffusion tensor imaging of neurodevelopment in children and young adults. NeuroImage 26, 1164–1173.

Sullivan, E.V., Adalsteinsson, E., Pfefferbaum, A., 2005. Selective age-related degradation of anterior callosal fiber bundles quantified in vivo with fiber tracking. Cereb. Cortex Adv. Access.

Sundgren, P.C., Dong, Q., Gomez-Hassan, D., Mukherji, S.K., Maly, P., Welsh, R., 2004. Diffusion tensor imaging of the brain: review of clinical applications. Neuroradiology 46, 339–350.

Tang, Y., Nyengaard, J.R., Pakkenberg, B., Gundersen, H.J.G., 1997. Age-induced white matter changes in the human brain: a stereological investigation. Neurobiol. Aging 18 (6), 609–615.